Axial Capacity of C900 PVC Pipe with Reinforced Gasketed Joints

Final Report

Submitted to:

Katie Ross

Denver Water

Prepared by:

J. L. Ramos

J. Hindman

B. Lucero

B. P. Wham

Center for Infrastructure, Energy, and Space Testing
Civil, Environmental, and Architectural Engineering
University of Colorado Boulder
Boulder, CO 80309

August 2020

University of Colorado Boulder
Center for Infrastructure, Energy, & Space Testing
Dept. of Civil, Environmental & Architectural Engineering
College of Engineering and Applied Science
428 UCB
Boulder, Colorado 80309-0428
t: 303.492.8221
CIEST@colorado.edu
website:www.colorado.edu/center/ciest

Table of Contents

List of Figures

List of Tables

1. Introduction

The scope of work included in this technical report was commissioned by Denver Water under the direction of Katie Ross. The report presents test results from a program designed to investigate the axial performance of nominal 6 in. (150 mm) diameter C900 pipe with reinforced gasketed joints. The work was undertaken in the Center for Infrastructure, Energy, and Space Testing (CIEST) which is affiliated with the Civil, Environmental, and Architectural Engineering Department at the University of Colorado Boulder.

The intent of this study is to impose externally applied axial loading to pressurized test specimens. The applied loading is representative of worst-case deformation conditions and derived from the significant ground deformations possible during earthquake-induced ground deformation such as landslides, fault rupture, and liquefaction-induced lateral spreading. As detailed, all tests were designed and performed in accordance with procedures and recommendations outlined by Wham et al. (2018).

The report is organized into five sections. Section 1 provides introductory remarks, including discussion of the test specimens and experimental overview. Section 2 presents the general axial test setup and experimental protocols. Section 3 discusses the axial tension tests. Section 4 discusses the cyclic test results. Finally, Section 5 provides a summary of test results.

1.1 Test Specimens

Pipe specimens consist of 6 in. diameter AWWA C900 polyvinyl chloride (PVC) pipe with standard bell and spigot joints. The joints are equipped with reinforced gaskets. The gaskets themselves provide the restraining mechanism to resist tension loads applied to the pipe. A typical joint under test is shown in Figure 1.1.

Figure 1.1. Example of a typical bell/spigot joint.

1.1.1 RieberLok Gasket

The RieberLok gasket, shown in Figure 1.2, can be used with any standard C900 bell and spigot joint. The factory gasket is pulled from the bell of the pipe and replaced with a reinforced RieberLok gasket according to the manufacturer's instructions and as shown in Figure 1.3 and Figure 1.4. The gasket is installed with the correct side (as marked on the gasket) facing toward the spigot.

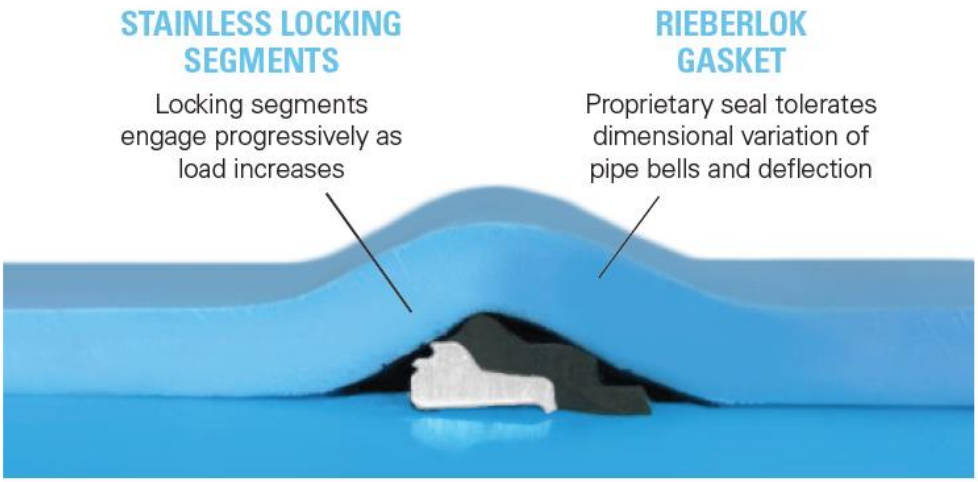

Figure 1.2. Illustration of RieberLok gasket (from manufacturer's data sheet: see references)

Figure 1.3. Replacing factory pipe gasket with reinforced RieberLok gripper gasket

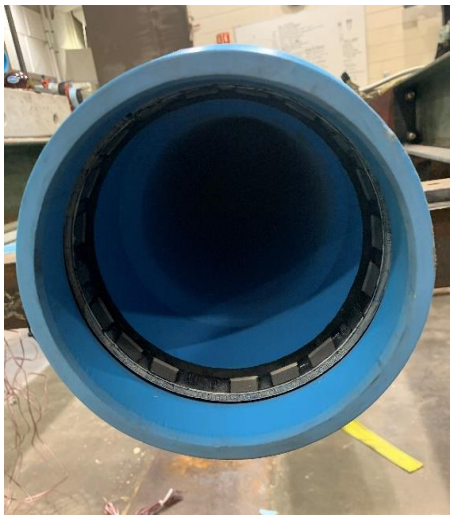

Figure 1.4. Fully seated RieberLok gripper gasket in the bell of a pipe

1.1.2 Diamond Lok-21 Pipe with Restraining Ring

Diamond Lok-21 pipe comes from the manufacturer fitted with a metallic restraint and a rubber gasket as shown in Figure 1.5. The gasket is not designed to be removed or replaced. It consists of a continuous steel ring with unidirectional serrated edges that allow the spigot to be inserted into the bell, but not pulled out.

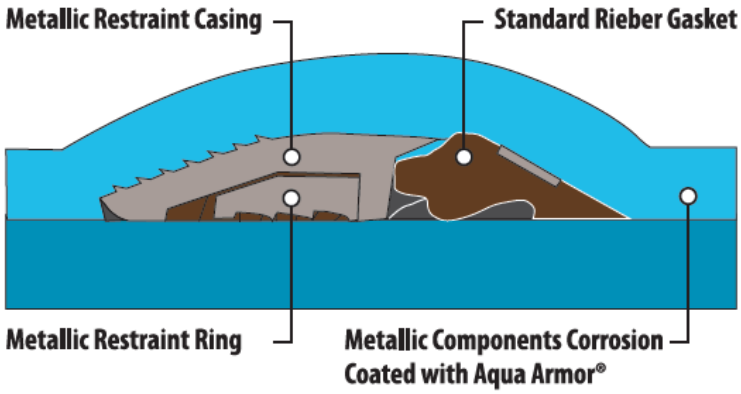

Figure 1.5. Illustration of Diamond Lok-21 gasket (from manufacturer's data sheet: see references)

1.2 Test Overview

All specimens tested herein are 6 in (150 mm) diameter pipe, commercially available and conforming to C900 (PVC) standards (AWWA, 2016). Pressure Class 235 (DR18) specimens are used for each test. Table 1.1 provides an overview of the test specimens and experiments performed. The Test ID represents the test type [pipe tension (PT) or pipe cyclic (PS)] and a unique numerical value specific to the sequence of testing performed at CIEST. The reinforced gasket type and approximate internal test pressure are also provided.

Table 1.1. Summary of Tests and Specimens

Test #	Test Type	Pipe Manufacturer	Gasket	Internal Pressure (psi)	Internal Pressure (kPa)
PT17	Axial Tension	NAPCO	RieberLok	71	490
PT18	Axial Tension	Diamond Plastics	Diamond Lok-21	65	450
PS19	Axial Cyclic	B-Vinyl Tech	RieberLok	66	455
PS20	Axial Cyclic	Diamond Plastics	Diamond Lok-21	64	440

2. Axial Test Setup and Protocols

This section provides a brief overview of the setup, procedure, and key experimental constraints associated with application of axial load to water distribution pipelines. The objective is to expose the system to external loading representative of moderate to severe ground deformation. All tests are designed and performed in accordance with procedures and recommendations provided by (Wham et al., 2018, 2019) Additional details regarding the CIEST test frame and setup details not included below are provided by (Ihnotic, 2019).

A 255.17 MTS actuator, 110-kip load cell, and load frame are used to apply tensile and compressive load to the test specimen. Figure 2.1 shows an image of a typical test setup and equipment. Figure 2.2 shows a dimensioned drawing of the test setup and equipment. The test specimens consist of nominal 6 in (150 mm) diameter pipe with bell and spigot joints. Internal water pressure is applied through a hydrostatic water pressure test system. A pressure regulator was used to maintain desired water pressure with manual valves available if necessary. A pressure transducer for measuring and recording pressure during the test is located at the upstream end of the 3/8-in. nominal hose supplying water pressure to the pipe.

Figure 2.1. Typical setup of pipe assembly in the load frame

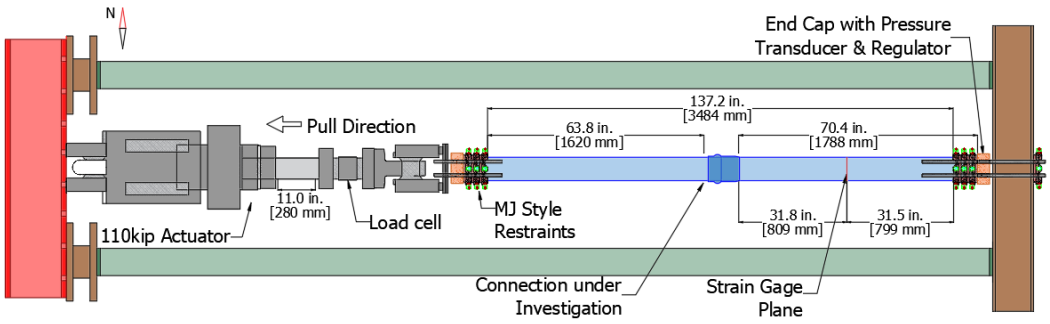

Figure 2.2. Dimensioned drawing of axial test setup

2.1 Specimen Installation Procedure

The pipe specimens are approximately 13 ft (4 m) long and consist of two 78 in. (1950 mm) long segments. The pipe is cut using standard field installation practices. Measurement marks are scribed at 1 in. (25 mm) increments on the factory-prepared spigot pipe end that is inserted into the bell joint.

For the RieberLok tests, the factory gasket is pulled from the bell of the pipe and replaced with a reinforced RieberLok gasket as shown previously in Figure 1.3 and Figure 1.4. The Diamond Lok-21 pipe comes from the manufacturer fitted with a reinforced gasket.

Three (3) 2006PV Megalug restraints are used at either end of the specimen to transfer externally applied axial load. Figure 2.3 shows the 3-restraint, end boundary condition at the loading end (west) and fixed end (east) of the specimen. Detailed procedures for end restraint assembly are provided by Ihnotic (2019).

The specimen is placed in the loading frame and the east and west connections are appropriately aligned with the 11 in. (279 mm) stroke actuator in its fully extended position (tension test) or a centered position (cyclic test). Lubrication (necessary for the gasket) is applied to the endcap gaskets and the inner diameter of the endcaps prior to the endcaps being tightened in place with six threaded rods (Figure 2.3). The threaded rods are also used to secure the east end to the load frame and the west end to the transfer plate on the end of the actuator. The threaded rods and nuts are arranged such that axial force from pressurization is resisted by the actuator, and thus recorded by the actuator load cell.

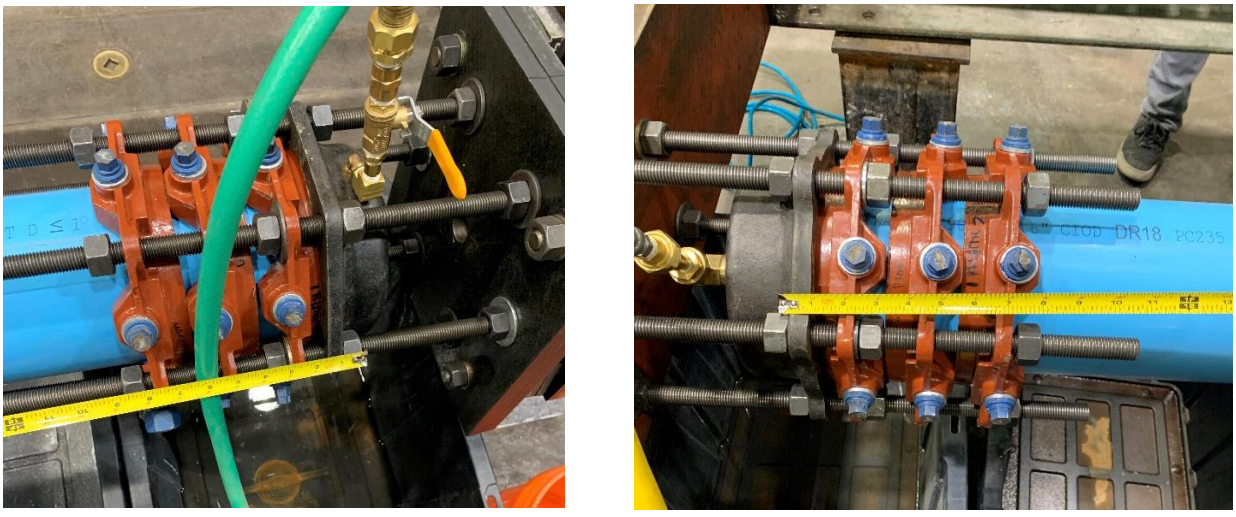

(a) Loading end (west) (b) Fixed end (east)

Figure 2.3. Pipe connections to loading frame

The east end cap is equipped with a port for the water pressurization hose. The west endcap includes a bleeder valve at the crown to remove air during filling of the pipe.

2.2 Instrumentation

Figure 2.4 shows a plan view of the tension test setup and key instrumentation. Force on the specimen is measured by a load cell attached to the piston of the hydraulic actuator. Actuator displacement is measured by an LVDT built into the actuator. A pressure transducer is installed on the water supply line to measure internal water pressure during each test.

Four string potentiometers (string pots) or linearly varying differential transducers (LVDTs) are attached to the specimen at several locations to measure axial displacements. A string pot/LVDT is used at each end of the specimen to measure relative movement between the pipe specimen and end restraints. Two additional string pots/LVDTs are installed at the center of the specimen to measure relative displacement between the spigot and the bell. Joint displacement measurements include stretching within the pipe itself between the measurement device mounting locations, but this quantity of displacement is considered negligible.

Two X-Y strain gauge rosettes are fixed to the exterior of the specimen at the east strain plane, designated as SG+36, as shown in Figure 2.4. The plane location is 36 in. (900 mm) away from the center of the joint and is also approximately halfway between the joint and end restraints. At the plane, the strain gauges are placed at the crown and invert. Gauges are oriented in the axial and circumferential pipe directions.

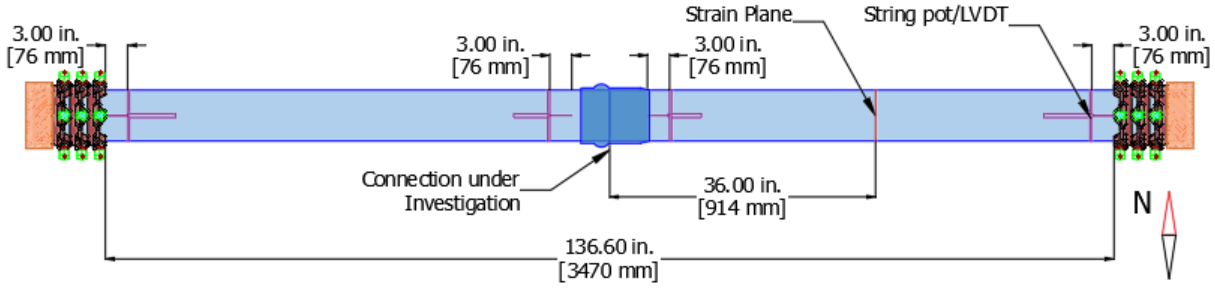

Figure 2.4. Specimen instrumentation

2.3 Test Procedure

The following section provides details of the test sequence, distributed into three parts: pretest, test sequence, and discussion of pause or stop criteria.

2.3.1 Pretest

Once the specimen is secured in the loading frame and the calibrated instrumentation is installed, the measuring systems are verified. The pipe is filled and pressurized with water, typically to about 65 psi (450 kPa), to check for leaks. Water is generally introduced into the specimen more than five hours before testing to ensure thermal acclimation to ambient laboratory conditions. Multiple pressurization sequences are completed to seat gaskets, verify readings of strain gauges and check axial force measured by the load cell. In each of the cycles the air bleed valve is opened to release any accumulating residual air. Prior to a pressurization sequence, the nuts between the loading frame and the endcaps are tightened, such that when the pipe is pressurized, the axial pressurization force can be measured by the load cell. During a pressurization sequence, the pipe is pressurized to approximately 65 psi (450 kPa) and back down to approximately 0 psi (0 kPa). After a series of pressurization sequences, data is collected, stored, and analyzed to ensure proper function of all measuring systems. The area surrounding the test frame is cleared of all tools and other objects. Once ready for the test, a pretest meeting is conducted to review installation conditions, instrumentation locations and expectations, and discuss safety equipment and concerns.

2.3.2 Tension Test Sequence

The test sequence is initiated by starting the data acquisition system and laboratory hydraulic systems. A data sampling rate of 4 Hz was used for all reported tests. The loading nuts at either end of the specimen are tightened to avoid any end movement due to pressurization. Water pressure is applied. Unless otherwise noted, the test is performed under displacement control at a rate of 1.0 in. (25 mm) per minute. Displacement is applied until the specimen is no longer capable of holding internal water pressure or until the maximum stroke of the actuator [11 in. (275 mm)] is reached. Once the test is completed, the data acquisition system is turned off, laboratory hydraulic systems are set to low pressure, and the data is backed up.

2.3.3 Cyclic Test Sequence

Cyclic testing was performed to determine if a reduction in maximum tensile joint strength occurs as a result of cyclic loading levels in excess of those that could be imposed by transient wave propagation. For

each test, alternating tensile and compressive loads were applied to the pipe specimen in increasing amounts of displacement. Cyclic loading was applied following guidelines of FEMA461, which discusses seismic load protocols for structural and nonstructural building components (Applied Technology Council, 2007). The imposed loading sequence is provided in Table 2.1. Each cycle began by loading in the tension direction. Displacement amounts shown are measured from the "zero" point established at the start of testing. After cyclic loading, the pipe specimen was loaded in tension until failure. All loads were applied at a displacement rate of 1 in. (25 mm) per minute.

Table 2.1. Cyclic Loading Sequence

Step	Displacement	Cycles
1	+/- 0.10 in. (2.5 mm)	3
2	+/- 0.20 in. (5.1 mm)	2
3	+/- 0.30 in. (7.6 mm)	2
4	+/- 0.40 in. (10.2 mm)	2
5	+/- 0.50 in. (12.7 mm)	2
6	Tension until failure	n/a

3. Axial Tension Test Results

The following sections provide results from axial tension tests performed on two different pipe connections.

3.1 Tension Test PT17 Results

North American Pipe Company (NAPCO) C900 pipe (PC235, DR18) with a RieberLok gasket installed in the bell and spigot joint was used for this test. Joint displacement was measured using a string potentiometer on the springline as shown in Figure 3.1(a). The string potentiometer body was mounted on the pipe about 2 in. (50 mm) from the start of the bell. The string attachment point was on the spigot pipe approximately 3 in. (75 mm) from end of the bell.

Figure 3.2 shows the pressure, actuator force, and actuator displacement relative to time during the test. Water pressure was held in the range of approximately 65 –75 psi (450 – 520 kPa) for the duration of the test prior to the failure of the joint. Pressure fluctuations before joint failure are due to increasing internal volume of the pipe during tensile loading and manual valve adjustments of the water supply. Tensile load was applied until the gasket failed to hold the spigot pipe in place. Failure was indicated by a loud pop, a sudden increase in joint displacement, drop in force, and significant water leakage from the joint. Images of the joint before and after the test are shown in Figure 3.1. The joint continued to leak significantly after failure. Additional displacement was applied to the specimen by the hydraulic actuator after the initial failure, shown in Figure 3.2(a), to pull the joint apart for inspection. However, the pipe was unable to hold pressure beyond ~450 sec, which was determined to be the termination point of the test.

Figure 3.3 shows the relationship between the actuator force and actuator displacement during the test. The maximum force was 24.6 kips (109 kN), which occurred just prior to the failure of the joint. The displacement of the actuator at failure was 2.01 in. (51.1 mm). Figure 3.4 shows the actuator force vs. the joint displacement. The joint displacement was 1.12 in. (28.4 mm) at the time of failure. The figures show

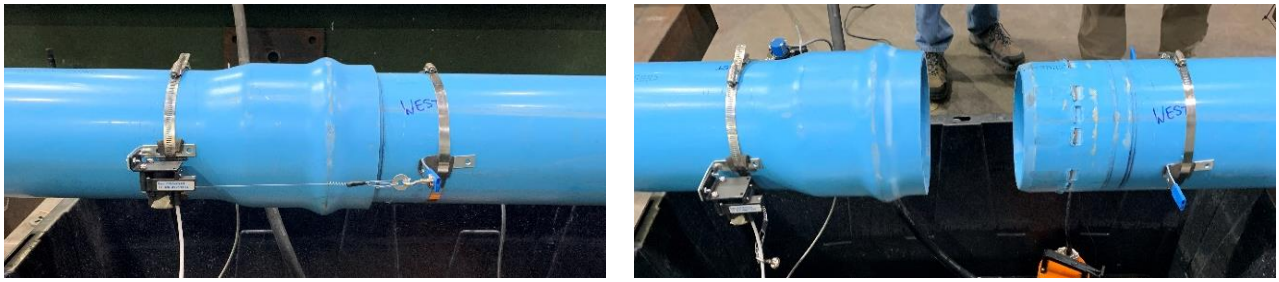

(a) (b)

Figure 3.1. Images of PT17, (a) before testing and (b) after failure

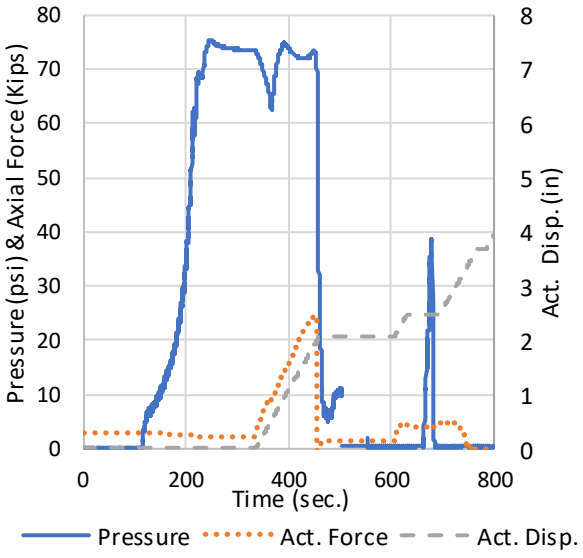

(a)

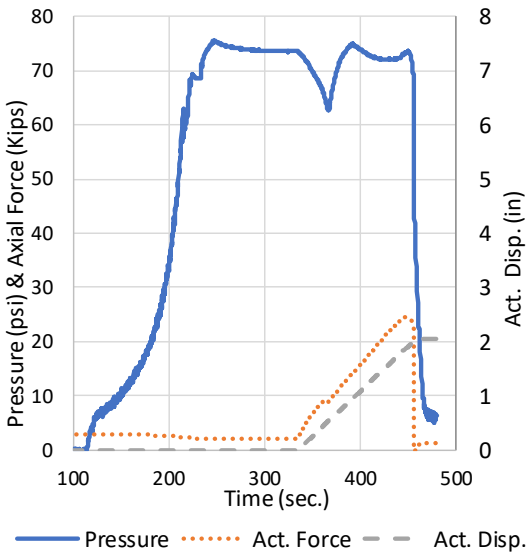

(b)

Figure 3.2. PT17 results for internal pressure, actuator force, and actuator displacement, vs. time: (a) entire test run, (b) detail data from start of loading to failure.

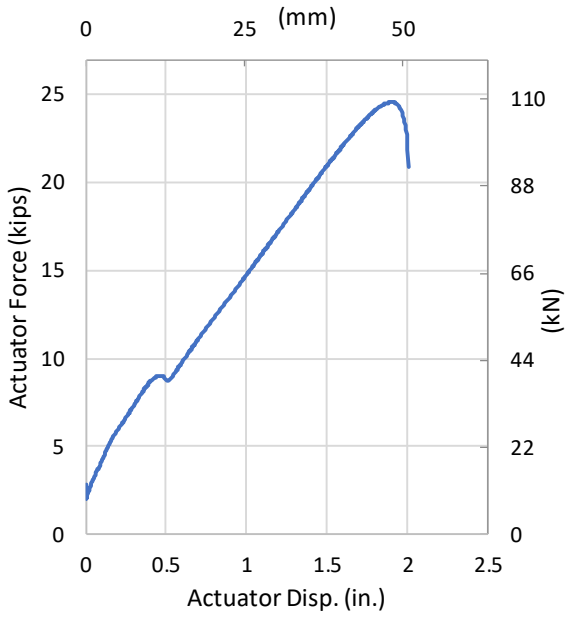

Figure 3.3. PT17 force vs. actuator displacement

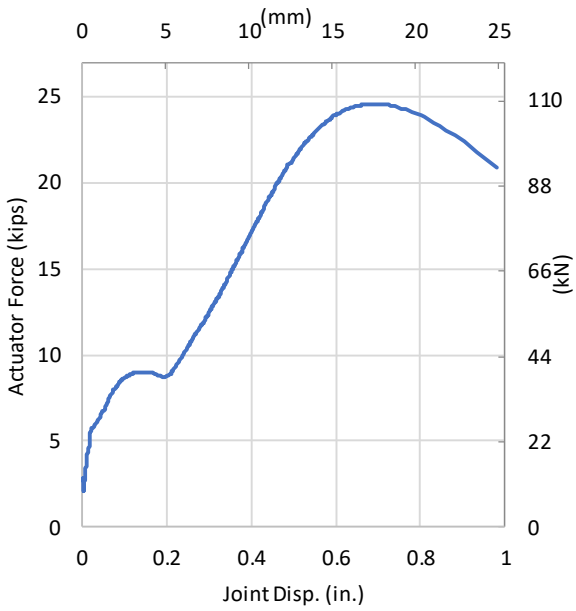

Figure 3.4. PT17 force vs. joint displacement

there was approximately 2 kips (9 kN) of axial tension load applied prior to the start of data acquisition due to the tightening of end restraint rods, which was captured in the load cell reading.

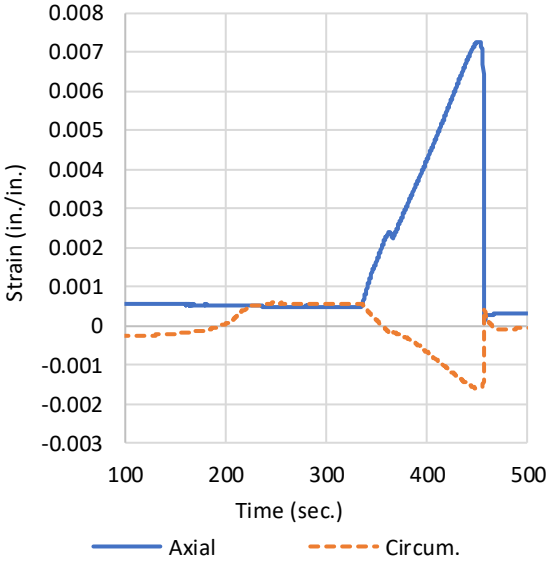

Figure 3.5. PT17 axial and circumferential strains vs. time

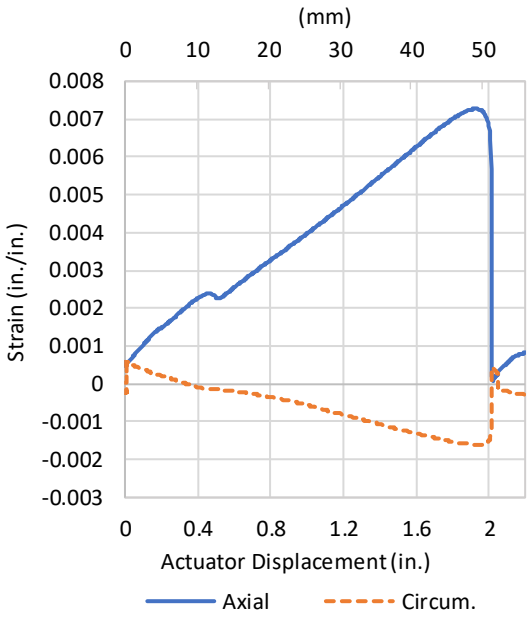

Figure 3.6. PT17 axial and circumferential strains vs. actuator displacement

The joint failed by the gripping teeth of the gasket gouging out material from the spigot pipe as can be seen in Figure 3.1(b). No cracks or breaks in the pipes were observed.

Figure 3.5 and Figure 3.6 show the axial and circumferential strains. Valid readings were obtained from only one strain gauge rosette. At the start of the test, the pipe was pressurized, and a resulting increase in circumferential strain was observed. Increasing tensile loading on the pipe resulted in increasing axial strain and reducing circumferential strain. The maximum axial strain at failure was 0.73% and the minimum circumferential strain was -0.16%.

3.2 Tension Test PT18 Results

Diamond Lok-21 PVC pipe with the as-received restraining-gasketed bell and spigot joint at the midpoint was used for this test. Joint displacement was measured using two spring pots located on the north and south pipe spring lines, as shown in Figure 3.7. The string pots and the string anchor points were fixed to the pipe approximately 3 - 6 inches (75 - 150 mm) on either side of the ends of the bell section. Water pressure was held at approximately 66 psi (460 kPa) during the application of load until failure. Tensile load was applied until the spigot pipe broke suddenly. An image of the joint after failure is shown in Figure 3.8 and Figure 3.9.

Figure 3.10 shows the actuator force, internal pressure, and actuator displacement relative to time. The maximum force was 32.6 kips (145 kN) at an actuator displacement of 2.11 in. (53.6 mm). Figure 3.11 shows the actuator force relative to actuator displacement. Figure 3.12 shows the actuator force relative to joint displacement. The average joint displacement was 0.37 in. (9.4 mm) at the time of failure. Failure occurred when the spigot pipe broke at the gasket with cracks propagating outwards from the joint. Figure 3.9 shows the failure of the spigot pipe inside the joint.

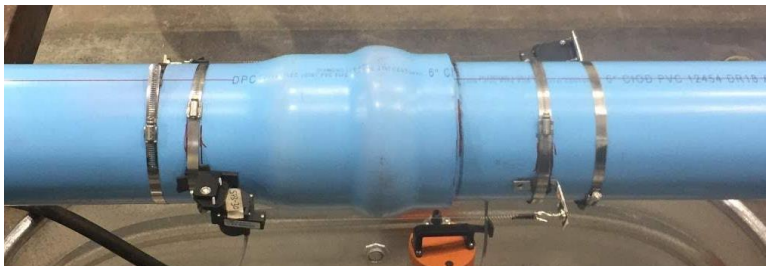

Figure 3.7. Pretest image of PT18

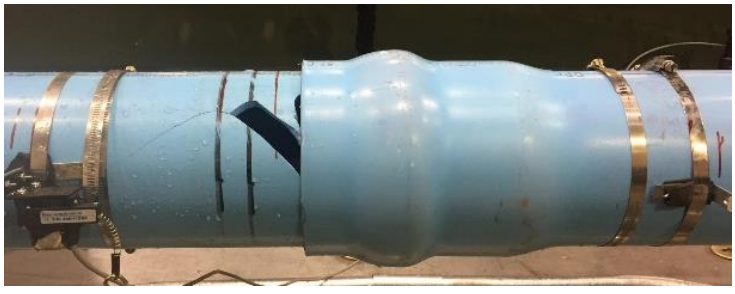

Figure 3.8. Post-test image of failure PT18 joint

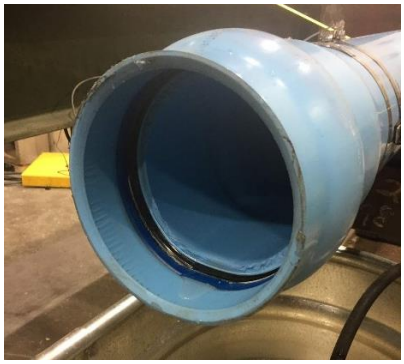

Figure 3.9. PT18 failure (note section of spigot circumferentially fractured inside joint)

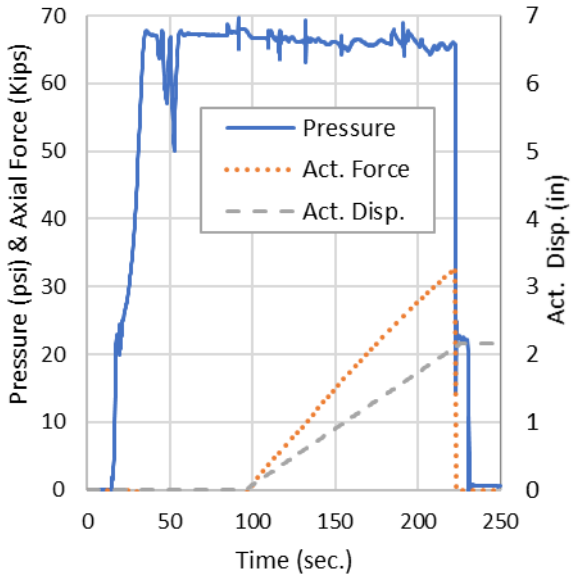

Figure 3.10. Specimen PT18 results for pressure, axial force, and actuator displacement vs. time

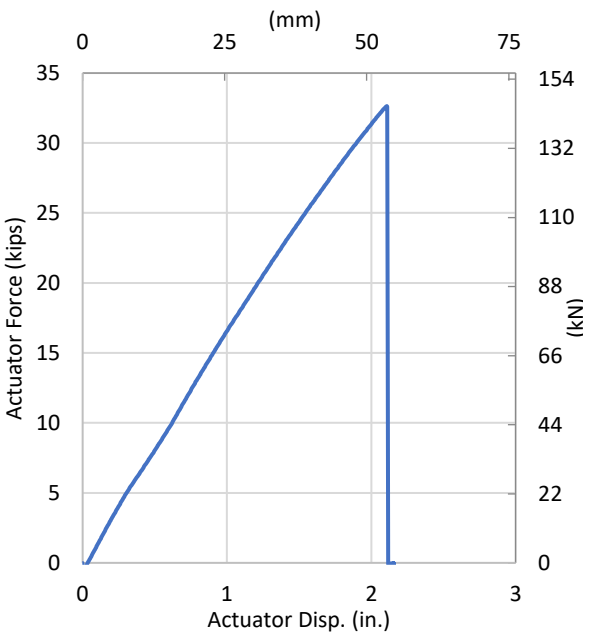

Figure 3.11. PT18 force vs. actuator displacement

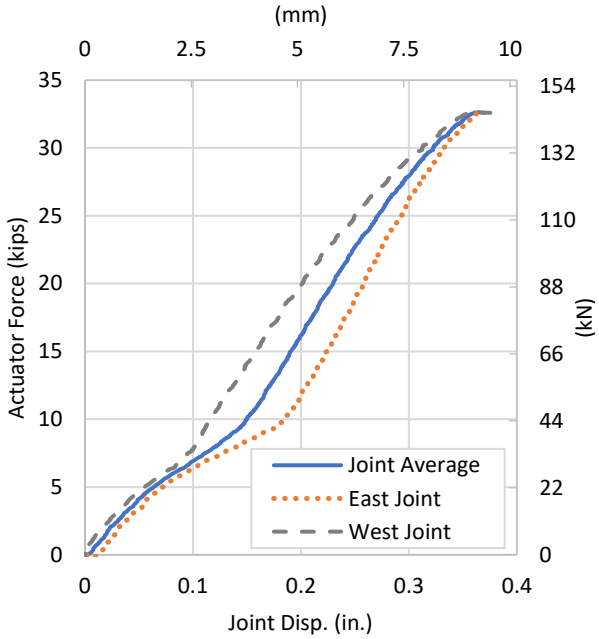

Figure 3.12. PT18 force vs. joint displacements

Figure 3.13 shows the axial and circumferential strain relative to time. Strain data is shown only from the strain gauges on the crown of the pipe. The gauges on the invert did not give valid data. At the start of the test, the system was fully pressurized, and an increase in circumferential strain was observed. Once loading began, the circumferential strains began to decrease, while the axial strains increased. Figure 3.14 shows the axial and circumferential strain relative to actuator displacement. The maximum axial strain at failure was 1.113% and the minimum circumferential strain was -0.270%.

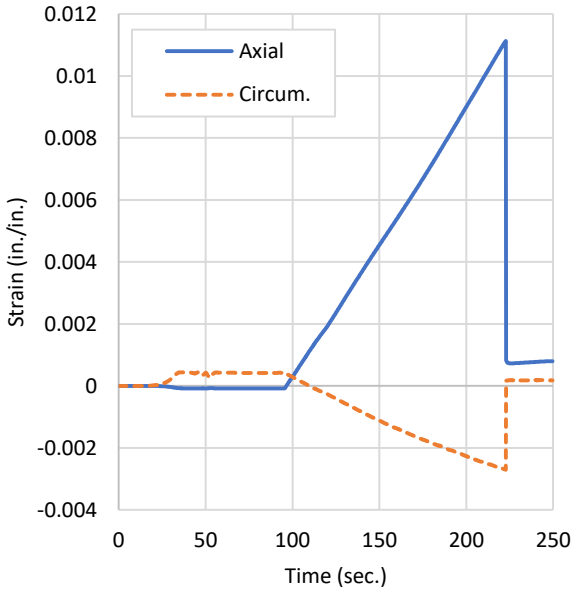

Figure 3.13. PT18 axial and circumferential strains vs. time

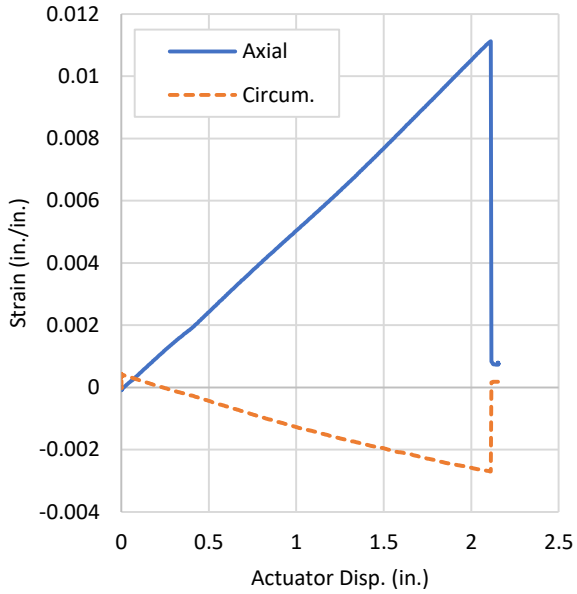

Figure 3.14. PT18 average axial and circumferential strains vs. actuator displacement

3.3 Tension Test Comparisons

Table 3.1 shows a summary of the axial tests performed. The Diamond Lok restrained bell was able to withstand greater axial tension force and joint displacement before failure than the RieberLok gasket. The Diamond Lok-21 joint failed by fracture of the spigot, whereas the NAPCO joint with a RieberLok gasket failed by movement of the pipe through the gasket, without pipe breakage.

Table 3.1. Summary of tension test results

Test #	Pipe-Connection	Max. Axial Force		Max. Axial Strain		Max. Act. Disp.		Joint Disp.	
		kips	(kN)	in/in	%	in	(mm)	in	(mm)
PT17	NAPCO- RieberLok	24.6	(109)	0.0073	0.73	2.01	(51)	1.12	(28)
PT18	Diamond Lok-21	32.6	(145)	0.0111	1.11	2.11	(54)	0.37	(9.4)

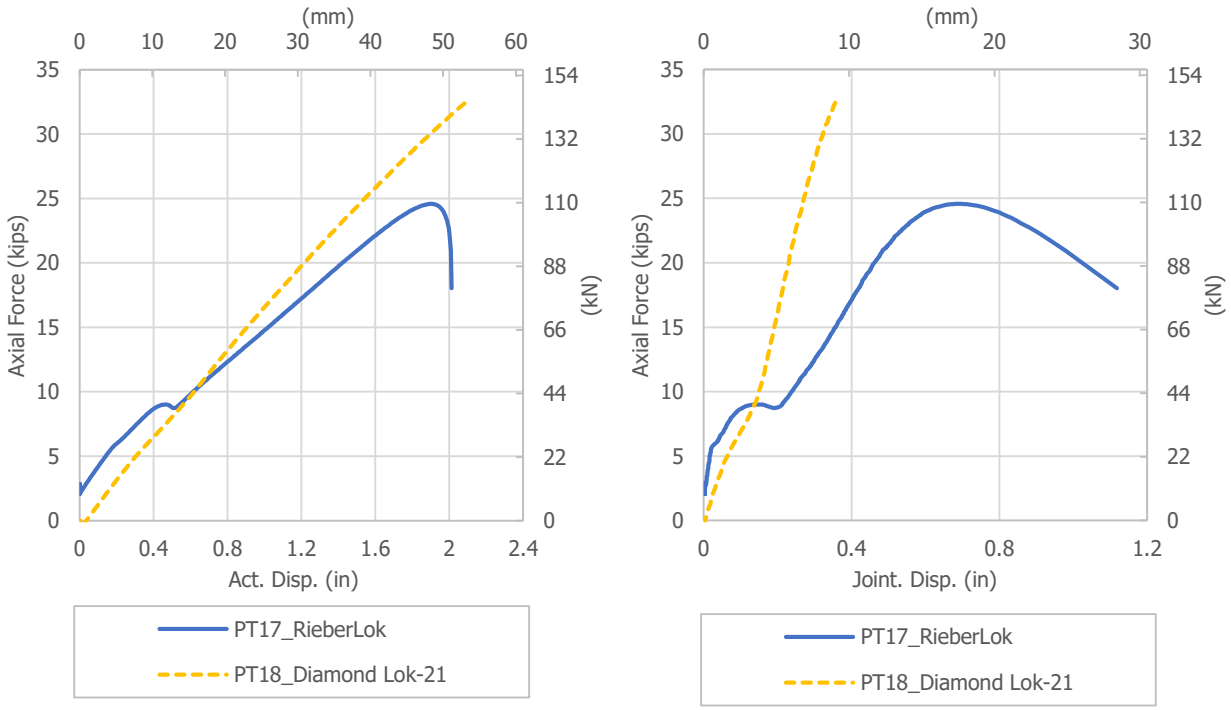

(a) (b)

Figure 3.15. Axial tension tests PT17 and PT18, force vs. (a) actuator and (b) joint displacements

4. Axial Cyclic Results

The following sections provide results from axial cyclic tension/compression tests performed on two different pipe connections.

4.1 Cyclic Test PS19 Results

B-Vinyl C900 pipe (PC235, DR18) with a RieberLok gasket installed in the bell and spigot joint was used for this test. Joint displacement was measured using two spring pots located on the north and south pipe spring lines, as shown in Figure 4.1. The string pots and the string anchor points were fixed to the pipe approximately 4 - 6 inches (75 - 150 mm) on either side of the ends of the bell section. Figure 4.2 shows the water pressure, actuator force, and actuator displacement relative to time during the test. The average water pressure during testing was approximately 68 psi (470 kPa), although changing the internal volume with cyclic loading and manual valve adjustments caused the pressure to fluctuate over the range of approximately 50 – 85 psi (340 – 590 kPa). An initial 9 loading cycles were performed with the actuator displacement inadvertently set too low by a factor of 10. The error was corrected (at approximately 600 seconds of test time as shown in Figure 4.2), and the test was started from the beginning following the load protocol listed in Table 2.1.

A minor leak at the joint started during the compression portion of the 6th loading cycle. The leak rate was up to several drops per second and then stopped as the load became tensile instead of compressive. This minor leaking happened again during the 7th cycle. The test was paused for inspection shortly after the peak of the tension portion of the 7th cycle. During the compression portion of Cycle 8, the leak became much larger, visually estimated to be about 1-2 gallons (4-8 L) per minute with an accompanying significant drop in water pressure. As the loading changed to tension, the water pressure recovered, and the leaking slowed significantly to about 0.5 gallon (2 L) per minute while the test was paused at the peak tension point of Cycle 9. During the compression portion of Cycle 9, the leaking increased again to about 1-2 gallons (4-8 L) per minute. However, as the loading changed to tensile, the leaking stopped. During the entirety of Cycles 10 and 11, only a few drops of water leaked from the joint during the compression portion of the cycle and no other leaking occurred until the failure of the spigot pipe at the end of the test.

Figure 4.3 shows the joint after failure. Failure occurred by circumferential fracture of the spigot at the location where the metal RieberLok teeth dig into the pipe. This failure is indictive of most/full mobilization of the pipe strength.

Figure 4.4 shows the relationship between the actuator force and actuator displacement. The maximum force was 23.8 kips (111 kN) and the maximum actuator displacement was 1.97 in. (50.0 mm). Figure 4.5 shows the actuator force vs joint displacement. The string potentiometer on the south side of the joint rotated during the final loading of the specimen, so data from this sensor was not included in the results.

Figure 4.6 shows the axial and average circumferential strains for the duration of the test. The data from the crown circumferential strain gauge appeared to indicate a faulty gauge or installation, so data from this channel was excluded. At the start of the test, the system was fully pressurized, and an increase in circumferential strain was observed. The frame also resisted the axial expansion of the pipe from the pressurization, resulting in a measured compressive force and a decrease in axial strain.

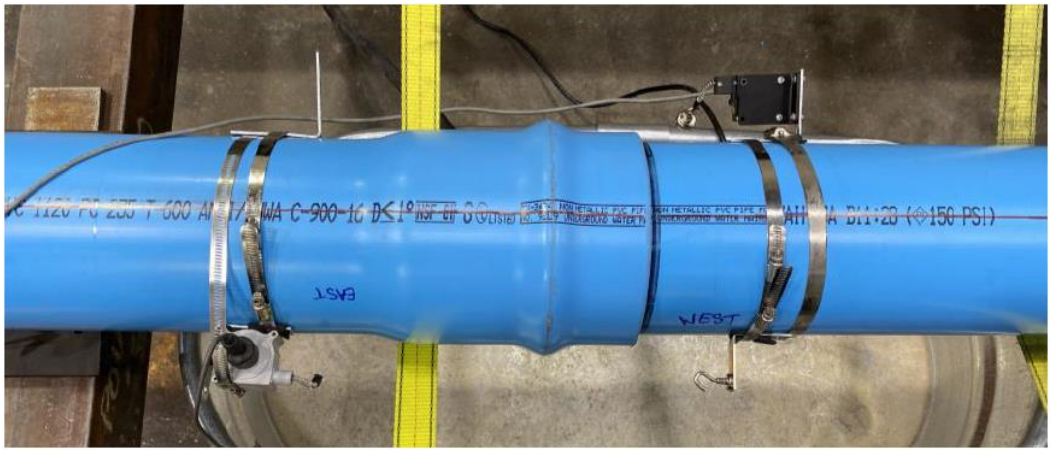

Figure 4.1. PS19 joint before testing

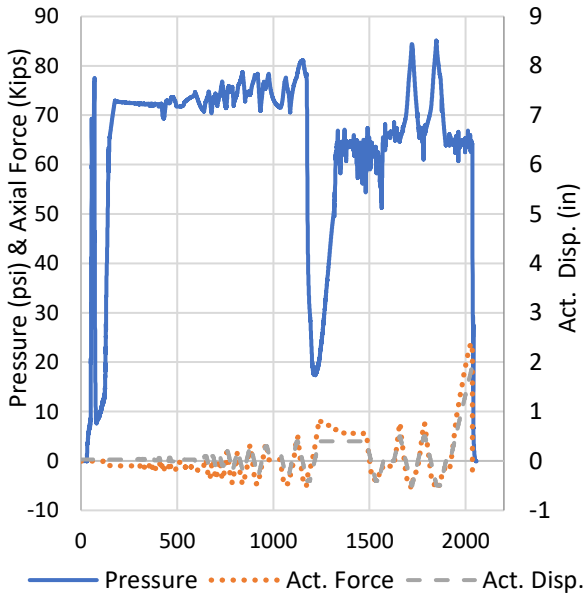

Figure 4.2. PS19 results for internal pressure, actuator displacement and axial force vs. time

(a) (b)

Figure 4.3. PS19 joint after failure, (a) broken spigot pipe, (b) inside bell

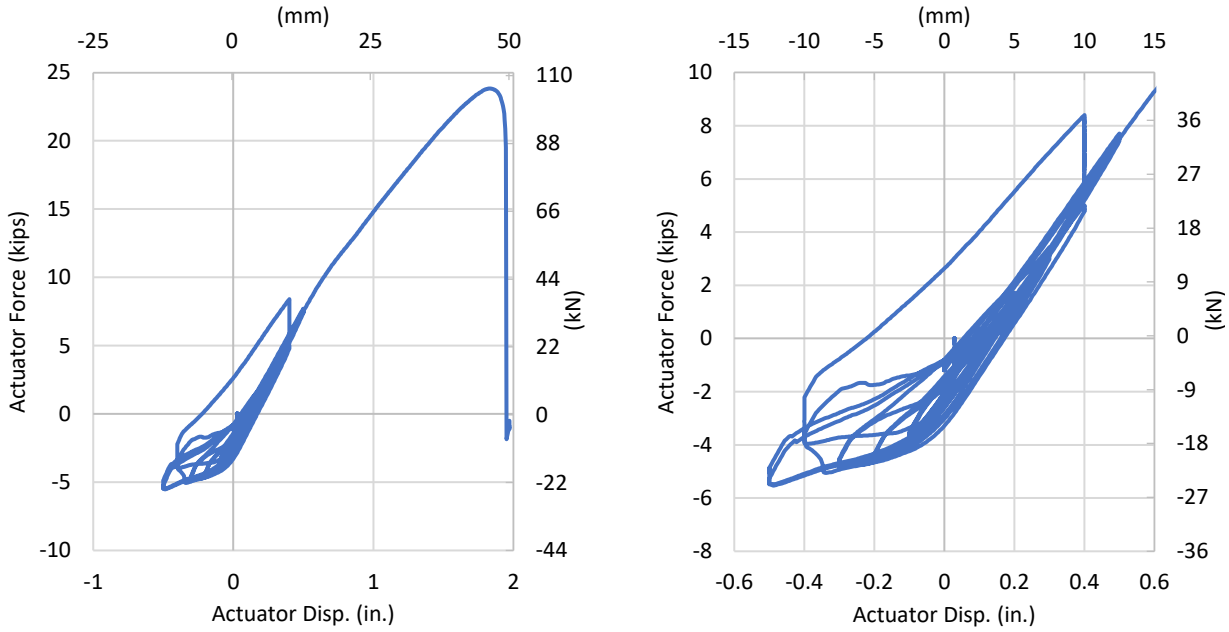

(a) Complete Test (b) Cyclic Loading detail

Figure 4.4 PS19 force vs. actuator displacement

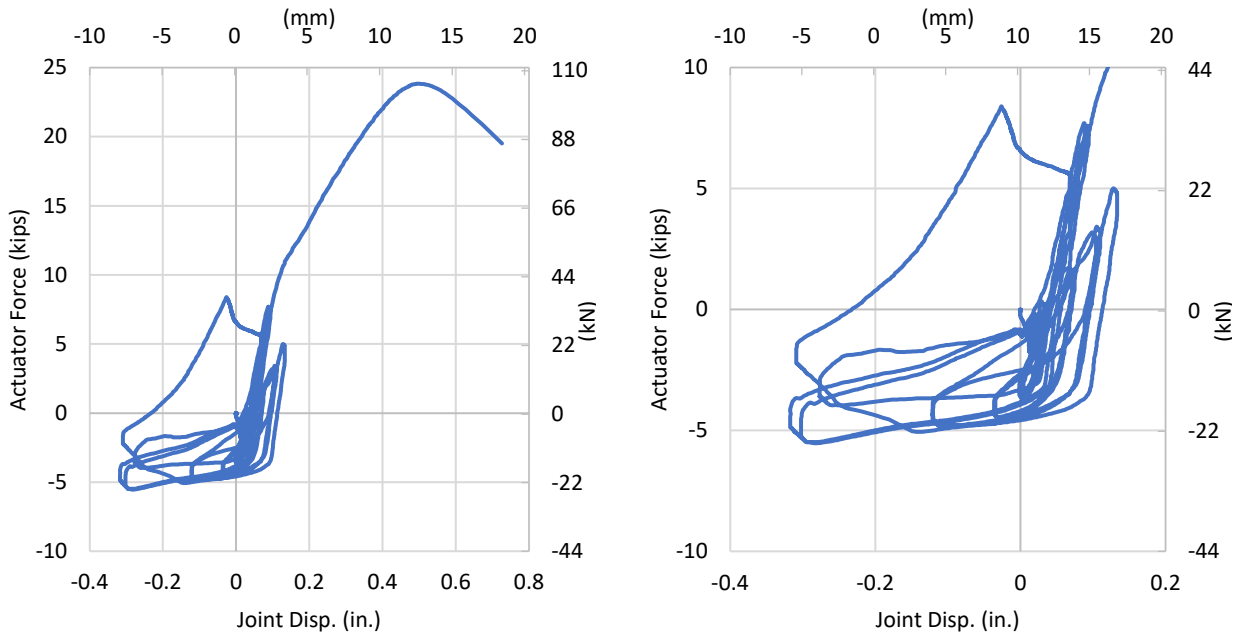

(a) Complete Test (b) Cyclic Loading detail

Figure 4.5. PS19 force vs. joint displacement

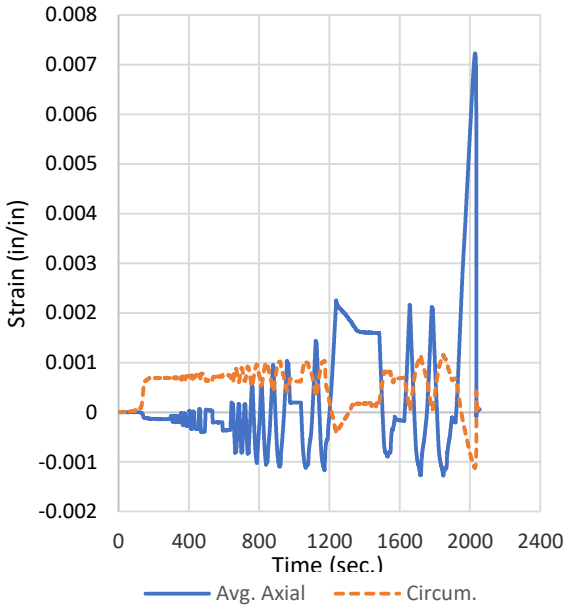

Figure 4.6. PS19 average axial and circumferential strains

4.2 Cyclic Test PS20 Results

Diamond Plastic's C900 pipe (PC235, DR18) with a Diamond Lok-21 gasket installed in the bell and spigot joint was used for this axial cyclic test. Joint displacement was measured using two string potentiometers on the spring line as shown in Figure 4.7(a). Each string potentiometer body was mounted on the pipe about 2.5 in. (60 mm) from the start of the bell. The string attachment point was on the spigot pipe approximately 6 in. (150 mm) from end of the bell. Water pressure was held in the range of approximately 60 –75 psi (410 – 520 kPa) for the duration of the test prior to the failure of the joint. Pressure fluctuations before joint failure are due to changing internal volume of the pipe during alternating tensile and compressive loading and manual valve adjustments of the water supply.

After cyclic loading, tensile load was applied until the pipe failed by breaking of the spigot pipe at the joint. Failure was indicated by a loud sound, a sudden increase in joint displacement and decrease in force, and significant water leakage from the joint. Images of the joint before and after the test are shown in Figure 4.7. Figure 4.8 shows the pressure, actuator force, and actuator displacement relative to time during the test. The maximum force was 30.2 kips (134 kN), which occurred just prior to the failure of the joint. The displacement of the actuator at failure was 1.78 in. (45.2 mm). Figure 4.9 shows the actuator force vs. the actuator displacement and the average joint displacement. The average joint displacement was 0.197 in. (5.00 mm) at the time of failure. The joint failed by circumferential fracture of the spigot at the location of the metal gasket teeth digging into the pipe as shown in Figure 4.10.

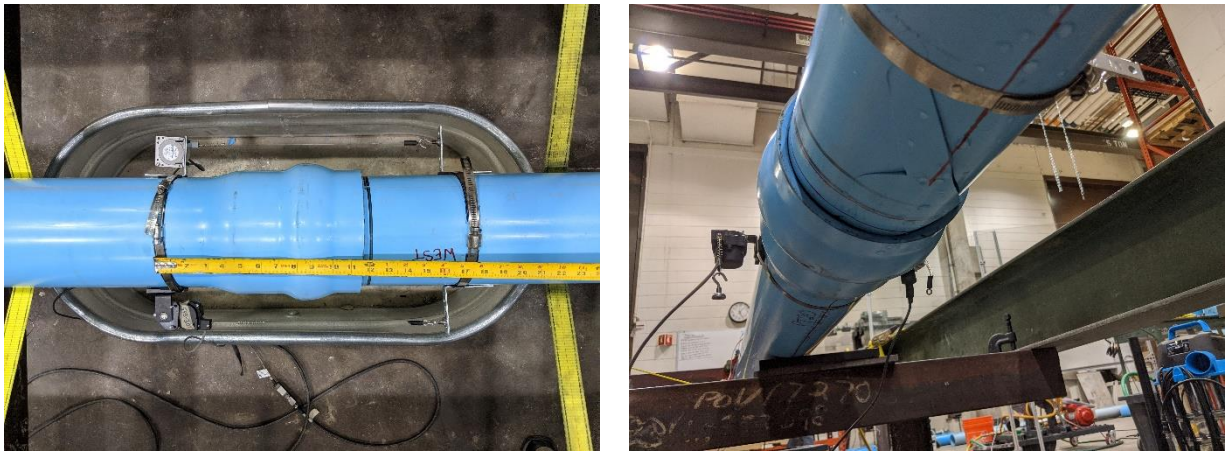

(a) (b)

Figure 4.7. Images of PS20, (a) before testing and (b) after failure.

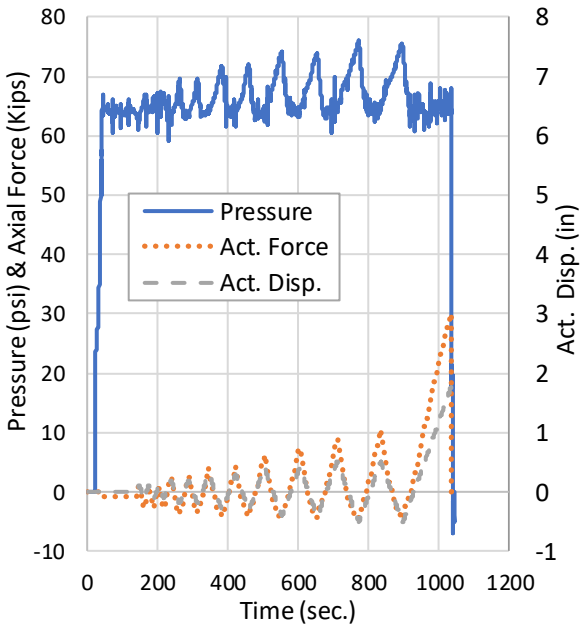

Figure 4.8. PS20 results for internal pressure, actuator displacement and axial force vs. time

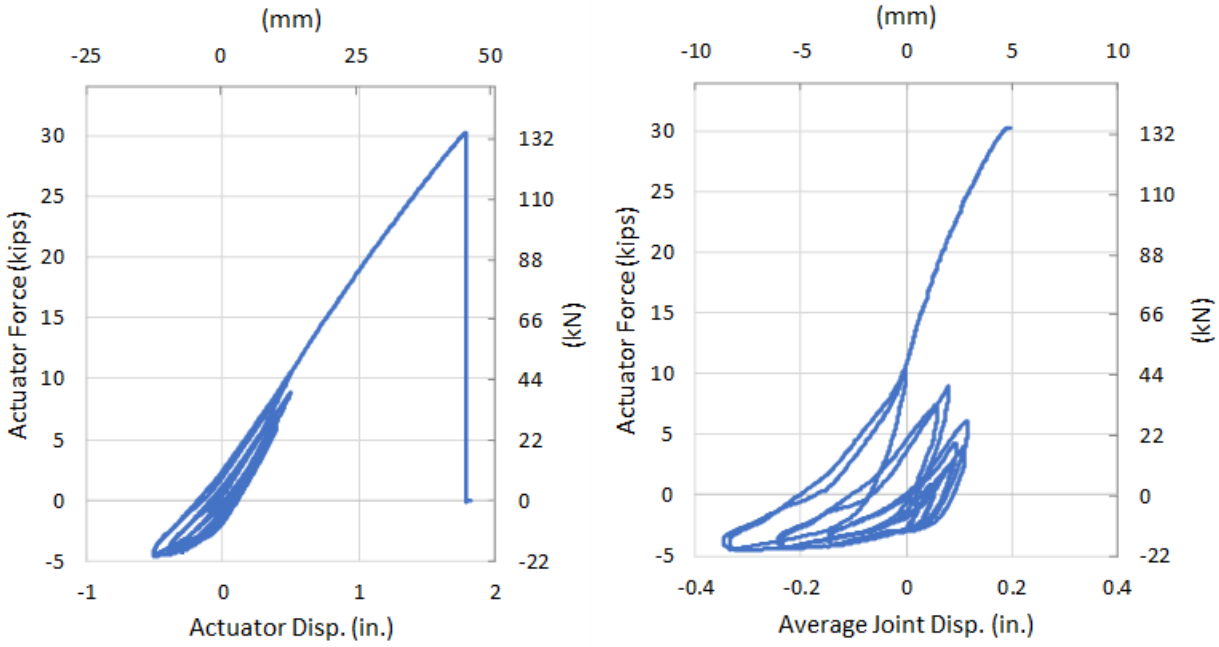

(a) (b)

Figure 4.9. PS20 force vs. (a) actuator displacement and (b) joint displacement.

Figure 4.10. PS20 joint failure.

Figure 4.11 shows the average axial and circumferential strains for the duration of the test. At the start of the test, the system was fully pressurized, and a resulting increase in circumferential strain was observed. The maximum axial strain was 0.925% and the minimum circumferential strain was -0.193%.

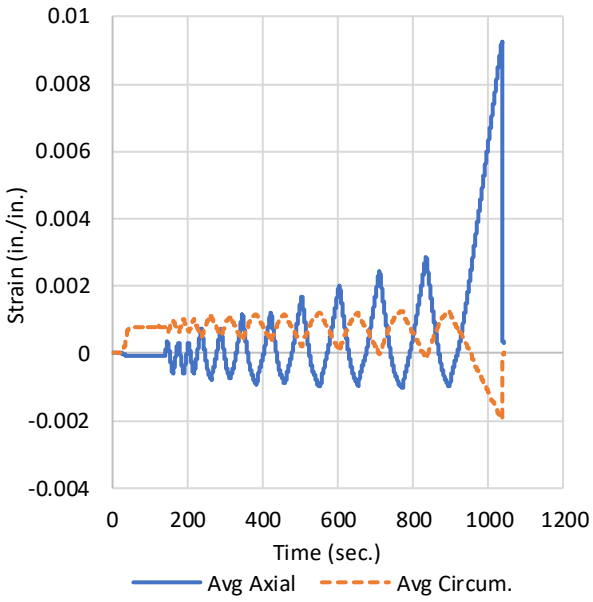

Figure 4.11. PS20 average axial and circumferential strains

5. Discussion and Conclusion

The following section provides comparisons of the four axial tests. Table 5.1 shows a summary of the primary test results. Figure 5.1 and Figure 5.2 show the relationship between axial force and actuator or joint displacement, respectively, for all four tests. Overall, both reinforced gasketed pipe joint products performed well under externally applied tensile and cyclic loading.

Table 5.1. Summary of all test results

Test #	Pipe-Connection	Max. Axial Force		Max. Axial Strain		Max Act. Disp.		Joint Disp.	
		kips	(kN)	in/in	%	in	(mm)	in	(mm)
PT17	C900- RieberLok	24.6	(109)	0.00727	0.727	2.01	(51)	1.12	(28)
PT18	Diamond Lok-21	32.6	(145)	0.01113	1.113	2.11	(54)	0.37	(9)
PS19	C900- RieberLok	23.8	(106)	0.00723	0.723	1.97	(50)	0.73	(19)
PS20	Diamond Lok-21	30.2	(134)	0.00925	0.925	1.78	(45)	0.20	(5)

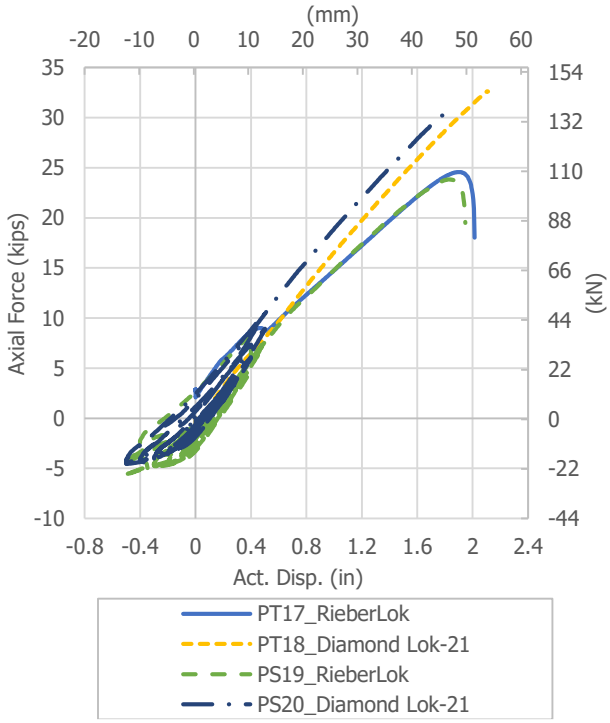

Figure 5.1. Force vs. Actuator Displacement, all four tests

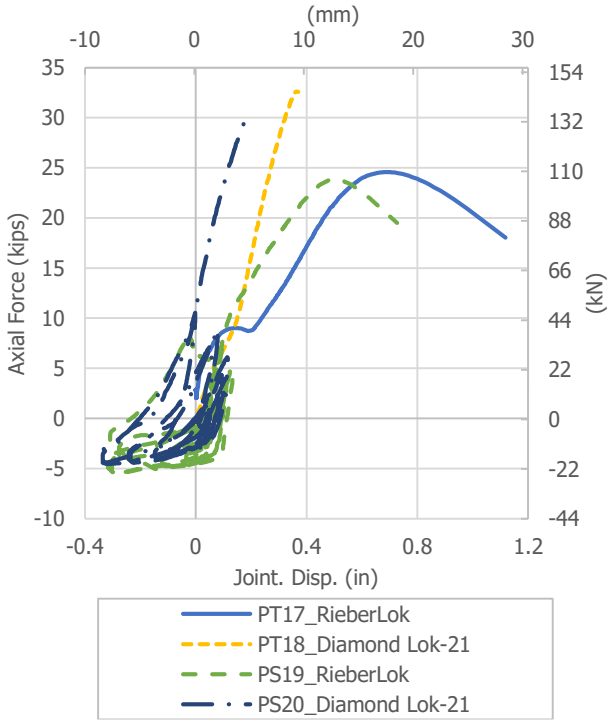

Figure 5.2. Force vs. Average Joint Displacement, all four tests

Failure mechanisms provide insight to pipe performance and evaluation. Both Diamond Lok-21 specimens failed in a similar manner, with a circumferentially fractured spigot remaining in the bell after the test

(Figure 3.9 and Figure 4.10). This failure mechanism indicates that a significant portion of the pipe barrel strength is mobilized before failure, generally a positive result, despite some minor longitudinal cracking of the spigot that might hinder repair efforts in the field.

Two different failure mechanisms are observed for the RieberLok specimens. In general, as the stainless locking segments (Figure 1.4) begin to indent the pipe spigot at significant levels of displacement (Figure 3.1(b)), they rotate and bend. Once one or more segments begin to buckle, the axial force begins to decrease under additional displacement. At 1.8 in. (45.7 mm) of imposed actuator displacement, softening of the axial load response of the RieberLok specimens can be observed (Figure 5.1 & 5.2). This reduction in load with additional displacement is associated with the joint failure mechanism. PT17 resulted in failure of the gasket, without fracture of the spigot or bell (Figure 3.1(b)), while PS19 failed similarly to the Diamond Lok-21 specimens, by circumferential fracture of the spigot. One explanation of this difference could be the use of two different PVC pipe manufacturers (NAPCO vs. B-Vinyl). More likely, the authors hypothesize cyclic loading caused these indentations to deepen, leading to propagation of circumferential fracture of PS19. Further evaluation and repeat tests may recommend reducing the maximum RieberLok joint displacement to the point of maximum load (~25% reduction of maximum joint displacement), rather than the instance of pressure containment loss (significant leakage under tension) reported herein.

Cyclic loading of the RieberLok specimen caused leakage during the compression cycles. However, under additional cycles, leakage stopped, and containment was preserved through failure. Since further cycles, at larger displacement/load levels, did not result in further significant leaking, it is assumed that the cyclic loading did not damage the gasket or joint, but only displaced the gasket such that the seal was partially compromised. This observation suggests the need to perform monotonic axial compression and/or additional cyclic tests to better understand this response, particularly for seismic applications.

Axial Load Capacity: The average maximum axial force applied to the specimens with RieberLok gaskets was 24.2 kips (108 kN). The RieberLok specimen that underwent initial cyclic loading reached a maximum force [23.8 kips (106)] that was 97% of the monotonically loaded specimen. Similarly, the average maximum force accommodated by the Diamond Lok-21 specimens was 31.4 kips (140 kN). The Lok-21 specimen that underwent initial cyclic loading reached a maximum force of 30.2 kips (134 kN), which was 93% of the monotonically loaded specimen. This comparison between monotonic and cyclic results indicate that, although some loss of axial tensile capacity is reported, a significant percentage of axial capacity (>90%) is preserved despite application of cyclic displacements in exceedance of movements expected due to typical operating conditions (normal pressure fluctuations, seasonal temperature changes, etc.).

The Diamond Lok-21 specimens accommodated larger axial loads than the RieberLok specimens, recording 33% and 27% greater capacity for the monotonic and cyclic tests, respectively. Overall, the Diamond Lok-21 specimens had 30% greater axial force capacity than the RieberLok specimens, considering averages of all four tests.

Axial Displacements: The average maximum joint displacement of the RieberLok specimens at failure [0.93 inch (24 mm)] was about 3 times greater than the Diamond Lok-21 joint displacement at failure [0.28 inch (7.1 mm)] (Figure 5.2). On the contrary, the Diamond Lok-21 specimens reached larger levels of axial strain in the pipe barrel (Table 5.1), due to the greater axial force capacity of the Diamond Lok-21 joint. The summation of these two mechanisms, both axial displacement accommodating strain and joint displacement, resulted in ultimate failure at relatively consistent values of imposed actuator displacement (Figure 5.1). In other words, the two specimen types were able to accommodate the imposed demand (actuator displacement) through a combination of two different primary pipeline capacities: joint displacement (RieberLok) and axial strain (Diamond Lok-21). Had the test specimens been shorter, the superior displacement capacity of the RieberLok gasket would have allowed the specimen to reach a larger imposed (actuator) displacement before failure relative to an identically sized Diamond Lok-21 specimen. On the contrary, if the test specimens were longer, (e.g., 18 ft on either side of the joint, similar to standard installation) the additional joint force capacity of the Diamond Lok-21 specimen would serve to develop axial strains over the entire pipe barrels and, therefore, based on the test results herein, outperform an identical RieberLok specimen.

Overall, both reinforced gasketed pipe joint products performed well under externally applied tensile loading. The results suggest these systems are viable options for regions prone to persistent soil movements and settlements, areas where unrestrained PVC joints may pullout over time.

Moreover, although inferior to some systems with regard to axial displacement capacity, the axial joint force capacity (AKA, connection force capacity) of the products tested are consistent with other jointed thermoplastic pipe products tested by the authors (Ihnotic et al., 2019; Price et al., 2018; Wham et al., 2017). Given the small profile of the internally restrained joint, compared to enlarged external joints that cause additional interaction with surrounding soil, the results suggest the systems tested may also be useful in areas of low to medium seismicity.

Despite the value of the enclosed program, additional testing would be useful to quantify variation in results among pipe products. As previously noted, axial compression tests would be useful to determine performance limits and leakage associated with the internal bell-spigot-gasket system. Four-point bending

tests of the pipe systems would also prove valuable to assess capacity to accommodate lateral (transverse) loading, particularly for potential seismic applications.

Acknowledgements

The authors wish to recognize the excellent effort of University of Colorado students and staff that made these experiments successful. Namely, the contributions of graduate students Corey Ihnotic, David Kyle Anderson and Hailey-Rae Rose; undergraduates David Balcells, Hayley Parnell, and Aldrich Valerian; and CIEST staff Kent Polkinghorne are gratefully acknowledged. Appreciation is extended to Denver Water for technical and financial support for this study, particularly Katie Ross.

References

Applied Technology Council. (2007). *FEMA 461: Interim Testing Protocols for Determining the Seismic Performance Characteristics of Structural and Nonstructural Components*. Redwood, CA: FEMA.

AWWA. (2016). *AWWA C900-16 Polyvinyl Chloride (PVC) Pressure Pipe and Fabricated Fittings, 4 in. through 60 in. (100 mm through 1,500 mm)*. Denver, CO: American Water Works Association. https://doi.org/http://dx.doi.org/10.12999/AWWA.C900.16

Ihnotic, C.R. (2019). *Seismic Evaluation of Hazard-Resistant Lifelines: Thermoplastic Pipes and Connections*. M.S. Thesis, Boulder CO: University of Colorado Boulder.

Ihnotic, C.R., Ramos, J.L., & Wham, B.P. (2019). "Seismic Evaluation of Hazard-Resistant Thermoplastic Pipe and RCT Coupling". Boulder, CO: Univeristy of Colorado Boulder.

Price, D., Berger, B.A., O'Rourke, T.D., Stewart, H.E., Wham, B.P., & Pariya-Ekkasut, C. (2018). *Performance Evaluation of iPVC Pipe under Earthquake-Induced Ground Deformation*. Ithaca, NY: Cornell University. Retrieved from https://lifelines.cee.cornell.edu/projects/

Wham, B.P., Argyrou, C., O'Rourke, T.D., Stewart, H.E., & Bond, T.K. (2017). "PVCO Pipeline Performance Under Large Ground Deformation". *Journal of Pressure Vessel Technology, 139*(1). doi.org/10.1115/1.4033939

Wham, B.P., Berger, B.A., Pariya-Ekkasut, C., O'Rourke, T.D., Stewart, H.E., Bond, T.K., & Argyrou, C. (2018). "Achieving Resilient Water Networks – Experimental Performance Evaluation". *Proceedings: Eleventh U.S. National Conference on Earthquake Engineering* (p. 11). Los Angeles, CA.

Wham, B.P., Ihnotic, C.R., Balcells, D., & Anderson, D.K. (2019). "Performance Assessment of Pipeline System Seismic Response". *Proceedings: JWWA/WRF/CTWWA Water System Seismic Conference*. Los Angeles, CA: JWWA/WRF/CTWWA Water System Seismic Conference.

"Lok-21™ Features & Benefits." *Diamond Plastics Corporation*, website: www.dpcpipe.com/docs/LOK21/LOK-21-Specifications.pdf.

"Pressure-Rated PVC Internal Restraint." *RieberLok*. Website: www.rieberlok.com/upl/downloads/resources/support-resources/rieberlok-tech-sheet-933d5dae.pdf.